Unsteady Transonic Flow Simulation on a Full-Span-Wing-Body Configuration

Guru P. Guruswamy*
Sterling Federal Systems, Inc., Palo Alto, California
and
Peter M. Goorjian†
NASA Ames Research Center, Moffett Field, California

The presence of a body influences both the aerodynamic and aeroelastic performance of wings. Such effects are more pronounced in the transonic regime. To account accurately for the effect of the body, particularly when the wings are experiencing asymmetric modal motions, it is necessary to model the full configuration in the nonlinear transonic regime. In this study, full-span-wing-body configurations are simulated for the first time by a theoretical method that uses the unsteady potential equations based on the small-disturbance theory. The body geometry is modeled exactly as the physical shape, instead of as a rectangular box, which has been done in the past. Steady pressure computations for wing-body configurations compare well with the available experimental data. Unsteady pressure computations when the wings are oscillating in asymmetric modes show significant influence of the body.

Introduction

THE computation of aerodynamic flow on full configurations is important for the efficient design of aircraft. To date the most advanced theoretical developments are for steady flows,[1,2] using the potential equations. Methods based on the more exact Euler/Navier-Stokes equations are still under development for computing steady flows about full aircraft.[3] Methods for unsteady computations are lagging in development relative to methods for steady computations, particularly for the transonic regime.

Accurate computations of unsteady forces on full aircraft configurations are required to predict aeroelastic characteristics of aircraft, especially in the transonic regime. In the transonic regime, unsteady aerodynamics are characterized by moving shock waves over aerodynamic bodies, such as a wing or fuselage. Aerodynamic forces are nonlinear, and they are very sensitive to changes in configurations that result from additional components and changes in flow parameters. For example, in the transonic regime, rapid variations in the pressure distributions with increasing Mach number result in an unsafe aeroelastic phenomenon called transonic dip,[4] and recent studies have shown that the aerodynamics of tip missiles can significantly influence the aeroelastic stability of wings.[5] Theoretical modeling for transonic flows requires the solution of time-dependent, nonlinear partial-differential equations that should be solved by a robust time-accurate method.

At the present time, the most advanced codes for transonic unsteady aerodynamics of wings are based on potential equations. One such unique code in use for both aerodynamic and aeroelastic analyses is the official Air Force/NASA XTRAN3S code, which uses the transonic small-disturbance (TSD) equation.[6,7] This code has the capability of modeling viscous boundary-layer interaction by using either the viscous wedge method or the lag entrainment method;[8] XTRAN3S is being used for routine aeroelastic applications for wings[9] and also to validate the development of unsteady codes based on the Euler/Navier-Stokes equations. The purpose of the present study is to extend further the capability of the XTRAN3S code to handle full aircraft with multiple components.[5]

Reference 10 presents an accurate method for computing steady transonic flows over wing-body configurations by using the modified TSD equation. In their method, the authors of Ref. 10 modeled the wing-fuselage configuration in a Cartesian grid system by constructing a grid so that points lay reasonably close to the fuselage. Because of the memory and speed limitations of computers available a decade ago, others resorted to a simplified approach that represented the fuselage as a box by using a slender-body theory.[11] Recently, a similar simplified approach was extended for unsteady flow computations of semispan wing-body configurations.[12] Since the simplifications are based on the subsonic slender-body theory, they can introduce inaccuracies for transonic flow computations. With present day computer resources that are about two orders of magnitude greater in memory and speed than computers available a decade ago, it is now practical to use the more accurate method of Ref. 10.

In the present study, the method of Ref. 10 is extended to compute unsteady flows over wing-fuselage configurations that model the actual shape of the fuselage and full wing span. In the present approach, pressures can be accurately computed at all points on the fuselage. Because of the full-span modeling of the wing in the present method, for the first time the unsteady transonic loads associated with asymmetric modes of aircraft and asymmetric configurations such as the oblique wing aircraft can be computed. Such computations are essential for accurate aeroelastic calculations.

The present work is done in conjunction with the further development of the official Air Force/NASA code XTRAN3S (Ref. 6), which is a general purpose code for computing unsteady transonics and the aeroelasticity of full aircraft. At present, this code can be used to compute flows over wings with tip-mounted missiles and with control surfaces. With the development presented in this paper, the code capability is close to computing flows on almost complete aircraft configurations. Because of the use of the TSD equation, the computa-

Presented as Paper 87-1240 at the 19th Fluid Dynamics, Plasma Dynamics, and Laser Conference, Honolulu, HI, June 8–10, 1987; received July 28, 1987; revision received Feb. 17, 1988.

*Principal Analyst. Associate Fellow AIAA.
†Research Scientist. Associate Fellow AIAA.

tional time is practical for computationally intensive aeroelastic calculations.

Steady and unsteady results for a full-span-wing cylinder configuration are presented for transonic Mach numbers. Present results are compared with earlier steady computations and experimental measurements. Results are also presented for wings oscillating with antisymmetric modes. Steady and unsteady pressures are computed for the RAE finite-wing-body configuration and steady pressures are compared with the available experimental data.[13] The effect of antisymmetric modes on the unsteady aerodynamics is illustrated for the RAE wing-body configuration. Although for the purposes of validation antisymmetric modes were used, the present development is valid for arbitrary asymmetric modes.

Formulation of Unsteady Transonic Flow Equations

The coordinate system used in this analysis is shown in Fig. 1. The three-dimensional, modified, small-disturbance, unsteady transonic equation of motion used in this analysis is given by[14]

$$A\phi_{tt} + B\phi_{xt} = (E\phi_x + F\phi_x^2 + G\phi_y^2)_x + (\phi_y + H\phi_x\phi_y)_y + (\phi_z)_z \tag{1}$$

where

$$A = M_\infty^2,\quad B = 2M_\infty^2,\quad E = (1 - M_\infty^2),\quad F = -(\tfrac{1}{2})(\gamma + 1)M_\infty^2,$$
$$G = -(\tfrac{1}{2})(\gamma - 3)M_\infty^2,\qquad H = -(\gamma - 1)M_\infty^2$$

The flowfield boundary conditions used are

Far downstream:

$$\phi_x + k\phi_t = 0 \tag{2a}$$

Far upstream:

$$\phi = 0 \tag{2b}$$

Far above and below:

$$\phi_z = 0 \tag{2c}$$

Far spanwise:

$$\phi_y = 0 \tag{2d}$$

Trailing vortex wake:

$$[\phi_z] = 0 \tag{2e}$$

$$[\phi_x + k\phi_t] = 0 \tag{2f}$$

where the [ ] denotes the jump in the quantity across the vortex sheet.

The thin-wing surface-flow tangency condition that is satisfied at the mean chord plane is given by

$$\phi_z = f_x + kf_t \tag{3}$$

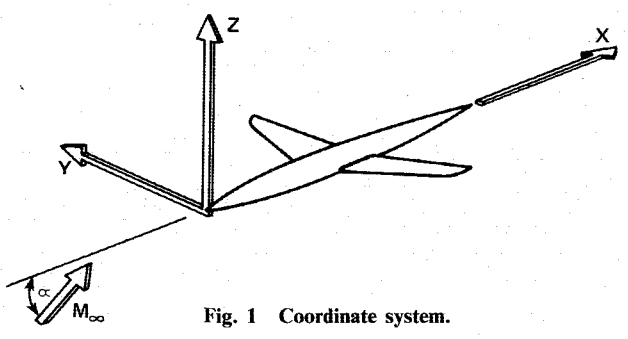

Fig. 1 Coordinate system.

where $f(x)$ denotes the airfoil surface function and $k = \omega c/U_\infty$ is the reduced frequency based on the full chord (ω is the frequency in rad/s, c is a reference chord length, and U_∞ is the freestream velocity).

The above equations are transformed so that a swept-tapered wing can be analyzed by using a finite-difference mesh that is aligned with the leading and trailing edges of the wing. The transformed equation is obtained by the Ames modified shearing transformation[7] solved by the time-accurate alternat-

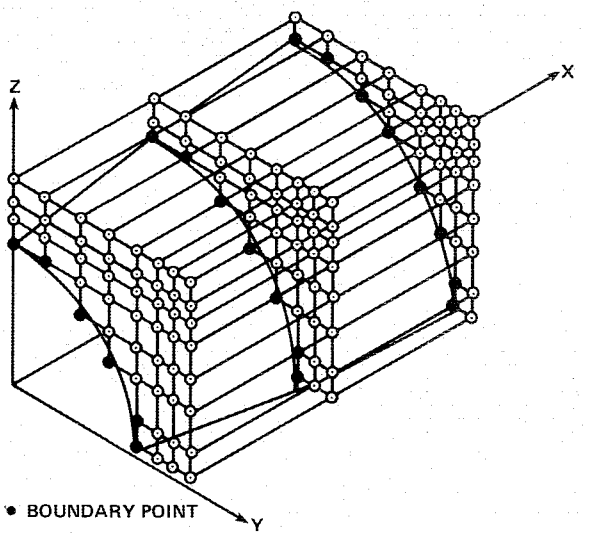

Fig. 2 Body boundary points.

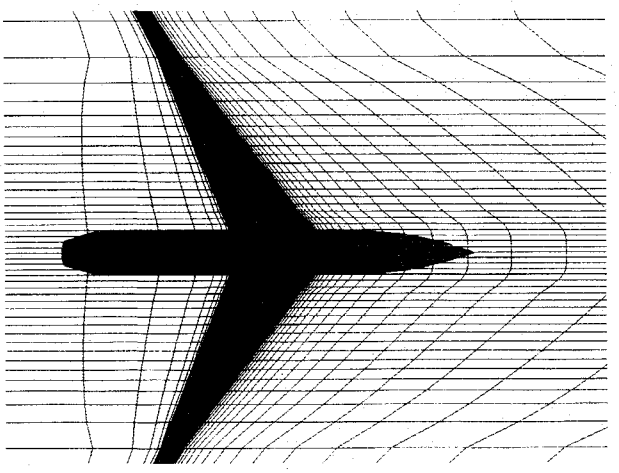

Fig. 3 Grid in x-y plane for the RAE wing-body configuration.

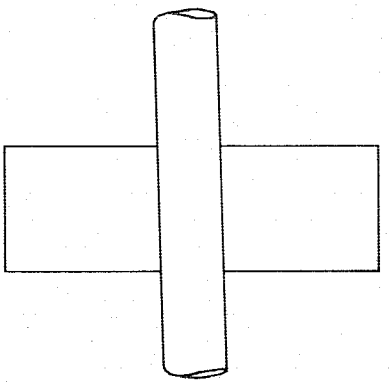

Fig. 4 Wing-infinite-cylinder configuration; aspect ratio = 3.56, NACA 65A006 airfoil.

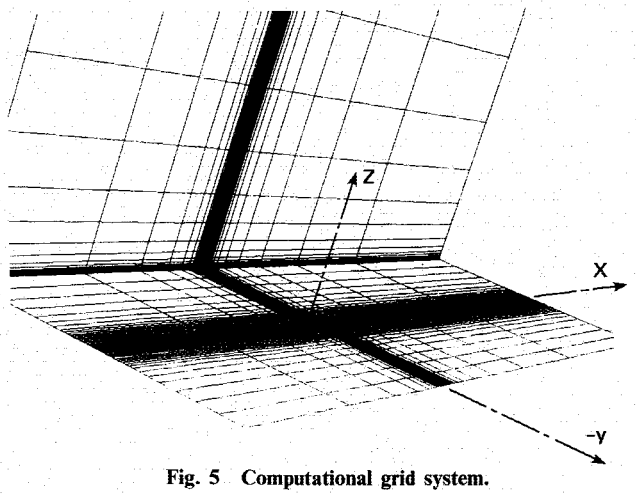

Fig. 5 Computational grid system.

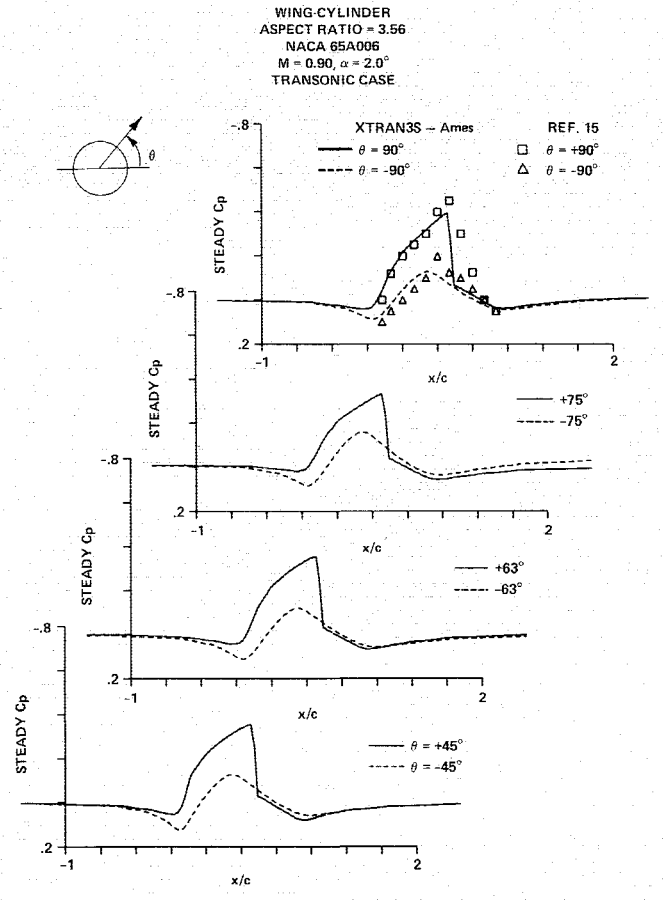

Fig. 6 Steady pressure distributions on the body of the wing-cylinder configuration.

ing direction implicit finite-difference scheme. The transformations that map a swept-tapered wing to a rectangular planform is given by

$$\xi = \xi(x,y) \tag{4a}$$

$$\eta = y \tag{4b}$$

$$\zeta = z \tag{4c}$$

where Eq. (4a) is obtained by using the Ames modified shearing transformation.[7] The resulting transformed equation

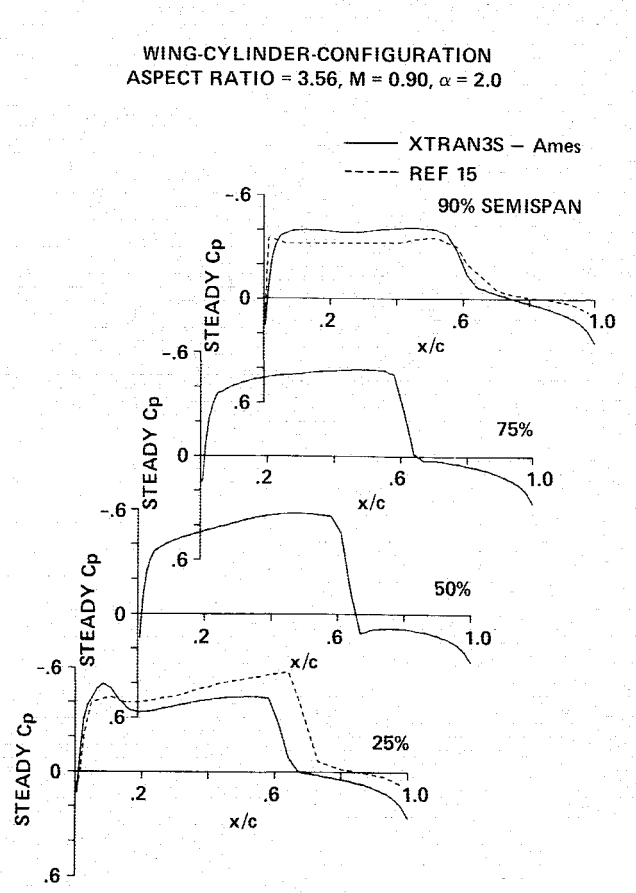

Fig. 7 Upper surface steady pressure distributions on the wing of the wing-cylinder configuration.

is given by

$$-(A\xi_x^{-1}\phi_t + B\phi_\xi)_t = [E\xi_x\phi_\xi + F\xi_x^2\phi_\xi^2 + G(\xi_y\phi_\xi + \phi_\eta)^2 + \xi_x^{-1}\xi_y(\xi_y\phi_\xi + \phi_\eta) + H\xi_y\phi_\xi(\xi_y\phi_\xi + \phi_\eta)]_\xi + [\xi_x^{-1}(\xi_y\phi_\xi + \phi_\eta) + H\phi_\xi(\xi_y\phi_\xi + \phi_\eta)]_\eta + (\xi_x^{-1}\phi_\zeta)_\zeta = 0 \tag{5}$$

The differencing procedure for Eq. (5) is an extension of the Murman-Cole type-dependent difference procedure applied to an arbitrary coordinate system. Type-dependent differences are used only to approximate derivatives in the streamwise direction corresponding to the x direction, and all other derivatives are approximated by central differences. This equation is solved by a time-accurate alternating direction implicit scheme.[7]

Aerodynamic Modeling of Fuselage

The fuselage is modeled as a body based on the small-disturbance theory. For a body described by the equation $g(x,y,z,t) = 0$, the small-disturbance-flow tangency boundary condition on the surface of the body becomes

$$kg_t + g_x + \phi_y g_y + \phi_z g_z = 0 \tag{6}$$

In the present method, the fuselage is treated in a rectangular mesh system, as shown in Fig. 2. The mesh is constructed so that points lie reasonably close to the fuselage surface. Depending on the mesh fineness, the grid points may lie either inside or outside of the fuselage surface. The boundary condition [Eq. (6)] is treated implicitly to give accurate and fast solutions as follows.

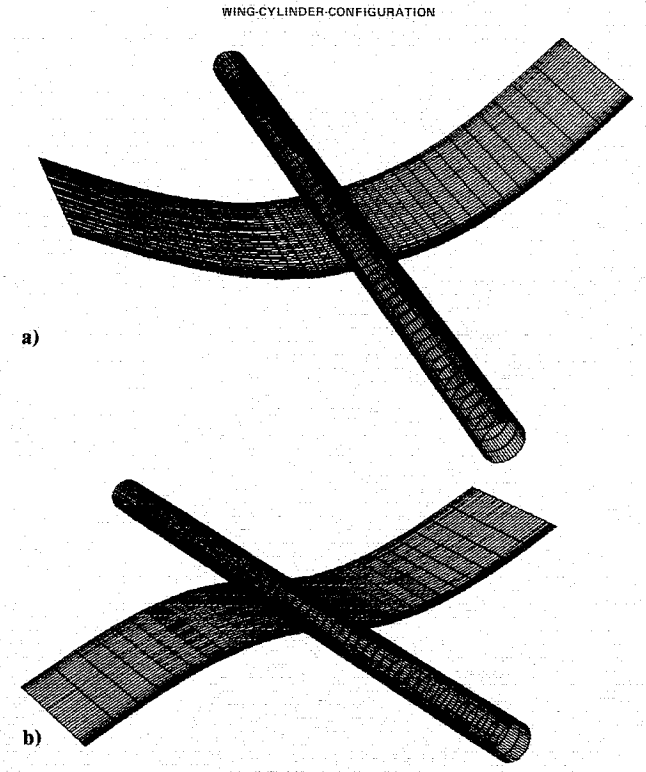

Fig. 8 Bending modes of wing-cylinder configuration: a) symmetric; and b) antisymmetric.

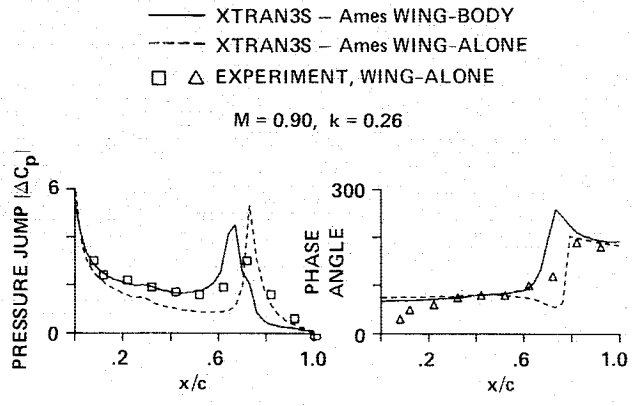

Fig. 9 Comparison of unsteady pressure jumps between theory and experiment.

The aerodynamic equation of motion, Eq. (1), is solved by the alternating direction implicit scheme using three sweeps. In the x sweep, the boundary condition [Eq. (6)] is imposed explicitly since it does not involve any derivatives of the potential in the x direction. In the y sweep, the ϕ_y term is implicitly treated, and the ϕ_z term is explicitly treated. In the z sweep, the ϕ_z term is implicitly treated, and the ϕ_y term is explicity treated. The two-point extrapolated differences are substituted for ϕ_y and ϕ_z at the boundary points.

The above approach needs an efficient grid-generation and body-boundary-point identification scheme. In this work, a numerical scheme that generates a grid for accurate modeling of a given wing-body configuration was developed and incorporated in XTRAN3S. This scheme gives a grid that is fine around the wing body and stretches smoothly far enough in the flowfield to reduce the effect of far-field boundary reflections. It clusters grid lines along the leading and trailing edges of the wing and gives adequate grid lines on the wing and the body. Figure 3 shows the grid in the x-y plane obtained by

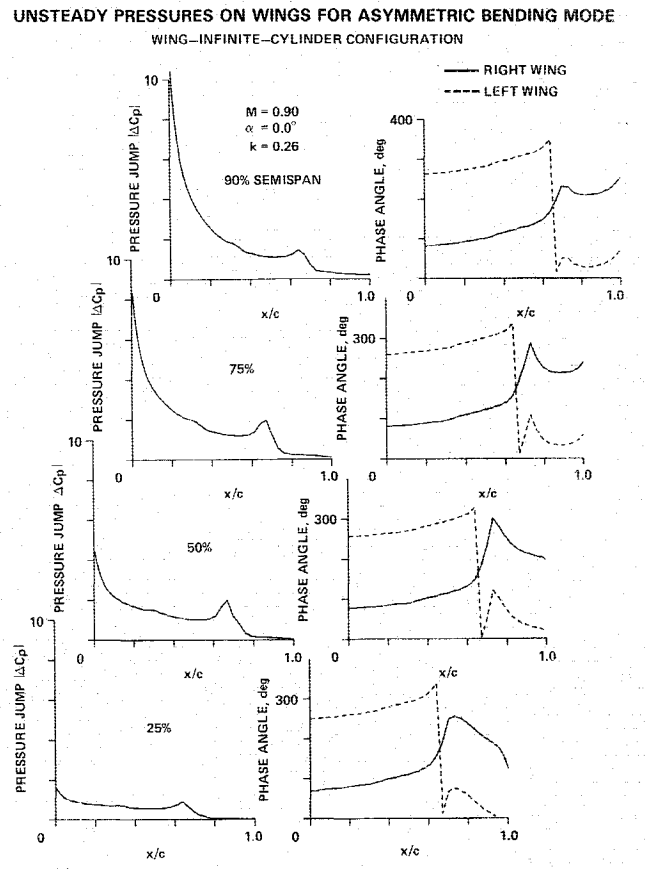

Fig. 10 Unsteady pressure jumps for antisymmetric modes at Mach number = 0.90.

the present grid-generation scheme for the RAE wing-body configuration. The boundary grid points on the body (Fig. 2) are automatically identified by the scheme without any user interface. In order to impose the boundary condition [Eq. (6)], which is in the Cartesian coordinate system, the grid-generation scheme generates a Cartesian physical grid near the body as shown in Fig. 3 for the RAE wing-body configuration. Thus, the metric term ξ_y is zero for all grid points on the body.

Results

Wing-Infinite-Cylinder Configuration

Steady and unsteady pressures were computed for a full-span-wing-infinite-cylinder configuration shown in Fig. 4. A Cartesian grid with 64 points in the x direction, 55 points in the y direction, and 40 points in the z direction was used in the analysis (Fig. 5). All computations were made for transonic flows with shock waves.

First, steady computations are shown for a wing-cylinder configuration at the transonic Mach number of 0.9. This configuration has a NACA65A006 wing cross section, an aspect ratio of 3.56, and a body of radius 1/10 of semispan. In Fig. 6, pressure distributions on the body are shown for four median angles. At 90 deg median angle (body symmetry line), the present results are compared with computations based on the classical steady TSD equation.[15] The comparisons are favorable. In Fig. 7, steady pressure distributions are shown for four span stations on the wing, and results are compared near the root and tip with those given in Ref. 15; again, the comparisons are favorable. Some discrepancies near the root could be due to differences in the TSD equations between Eq. (1) used in the present work and that used in Ref. 15. Reference 15 uses the classical TSD equation, whereas in the

present approach the more-accurate, modified TSD equation is used, which includes crossflow coupling terms in the nonlinear terms of Eq. (1).

Next, unsteady computations are made for a wing-cylinder configuration. All computations are made at a transonic Mach number of 0.9 and at a reduced frequency $k = 0.26$. This configuration has a wing with a 6%-thick parabolic arc section, an aspect ratio of 3.28, and a body radius of 1/10 of semispan. The aspect ratio of the wing without the body is 3. This configuration was selected to compare the present unsteady results with the unsteady wind-tunnel pressure measurements on an isolated wing of aspect ratio 3 oscillating in its first bending mode.[16]

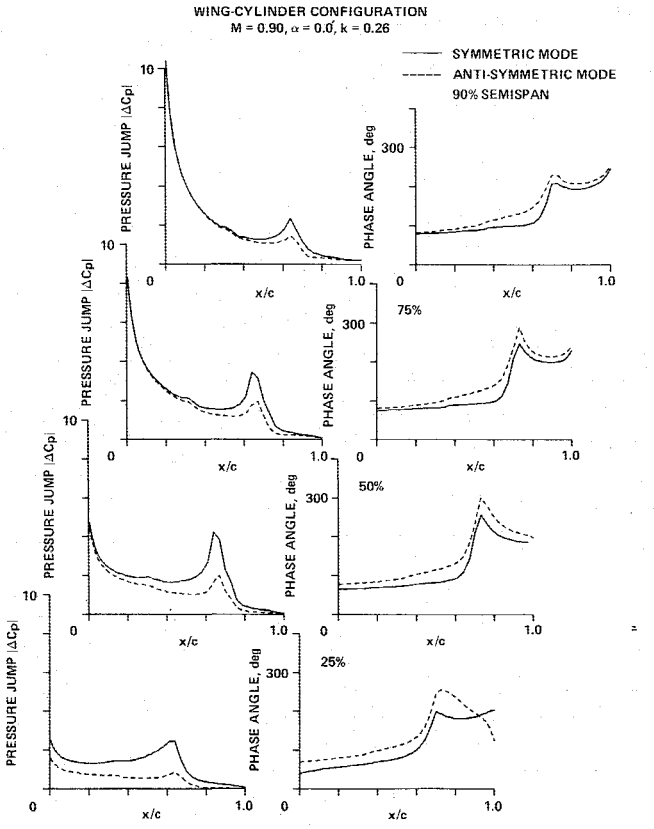

Fig. 11 Comparisons of unsteady pressure jumps between symmetric and antisymmetric modes.

Figures 8a and 8b show the symmetric and antisymmetric first-bending modes of the wing, respectively. The magnitude and corresponding phase angle of the unsteady pressure jumps at the 50% semispan station are shown for this wing-body configuration in Fig. 9. In the same figure, since there is no experimental unsteady pressure data for the wing-cylinder configuration, experimental results from Ref. 16 for the equivalent isolated wing mounted on a wall are shown. The presence of the body shifts the magnitude and phase curves without changing the general trend. For comparisons, results from XTRAN3S for the wing without the body are also shown in Fig. 9.

In Fig. 10, the unsteady pressure results are shown for the right and left wings when the wings are undergoing antisymmetric modal motions. Because of antisymmetry, the phase angle of the left wing is shifted by 180 deg from that of the right wing. However, the magnitudes remain the same for both wings. This verifies the accuracy of the present modeling. The unsteady pressure results for four span stations on the right wing are shown in Fig. 11 for the symmetric and antisymmetric bending modes. The antisymmetric mode has smaller pressure magnitudes and greater phase-angle shifts than the symmetric mode. Such differences can significantly influence the aeroelastic characteristics of aircraft.

Finite-Wing-Body Configuration

Steady and unsteady pressures are computed for the RAE wing-body configuration shown in Fig. 12. This configuration has a wing that is a 9%-thick RAE 101 airfoil in cross section, an aspect ratio of 6, and a wing leading-edge sweep angle of 36.65 deg. A grid with 82 points in the x direction, 55 points in the y direction, and 40 points in the z direction (Fig. 3) is used in the analysis. All computations are made at the transonic Mach number of 0.9 with shock waves.

In Fig. 13, pressure distributions on the body are shown for four median angles from both XTRAN3S and the experiment.[13] The comparisons are favorable. In Fig. 14, pressure distributions on the wing are shown for four span stations from both XTRAN3S and the experiment;[13] again, the comparisons are favorable, particularly for the 25% semispan station, which is very close to the body.

Unsteady pressure computations were made for the wings oscillating in symmetric and antisymmetric modes. Both first-

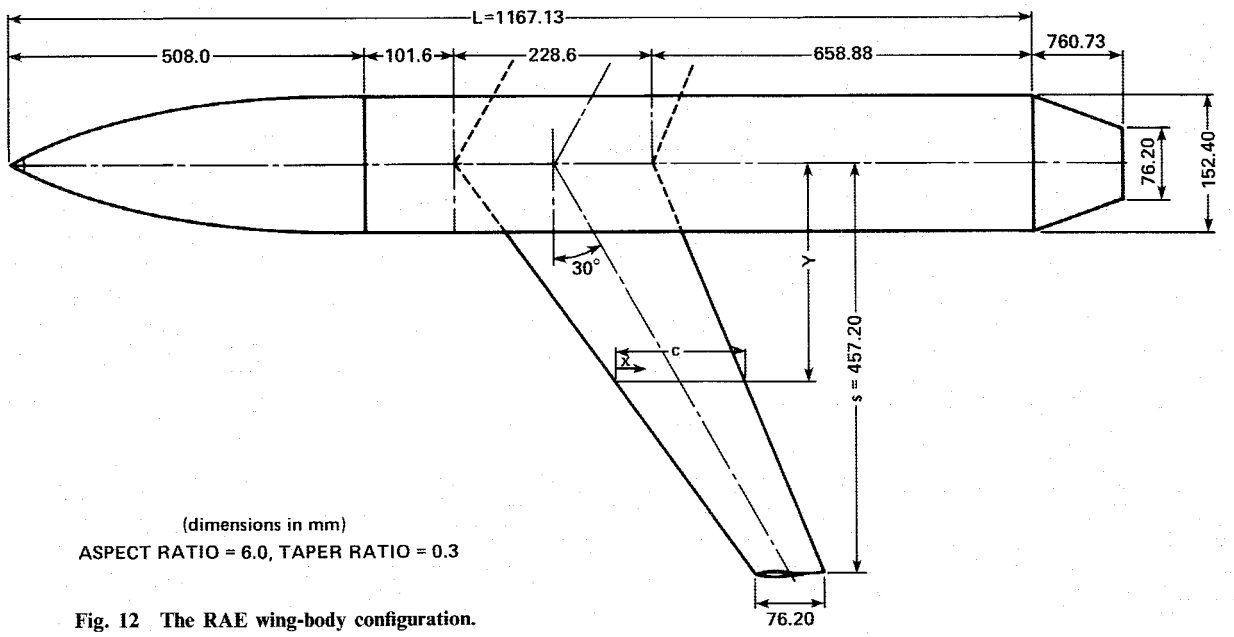

Fig. 12 The RAE wing-body configuration.

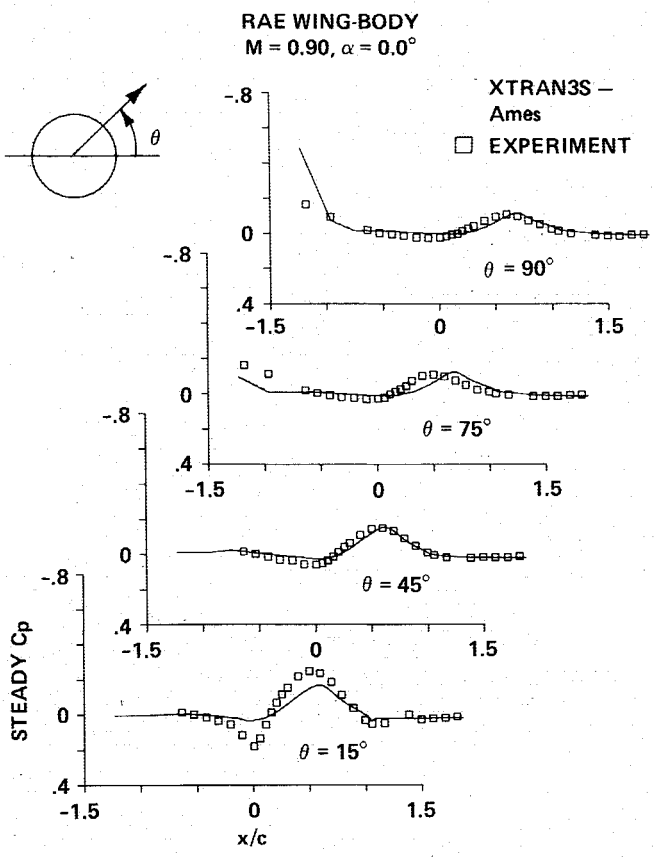

Fig. 13 Steady pressure distributions on the body of the RAE wing-body configuration.

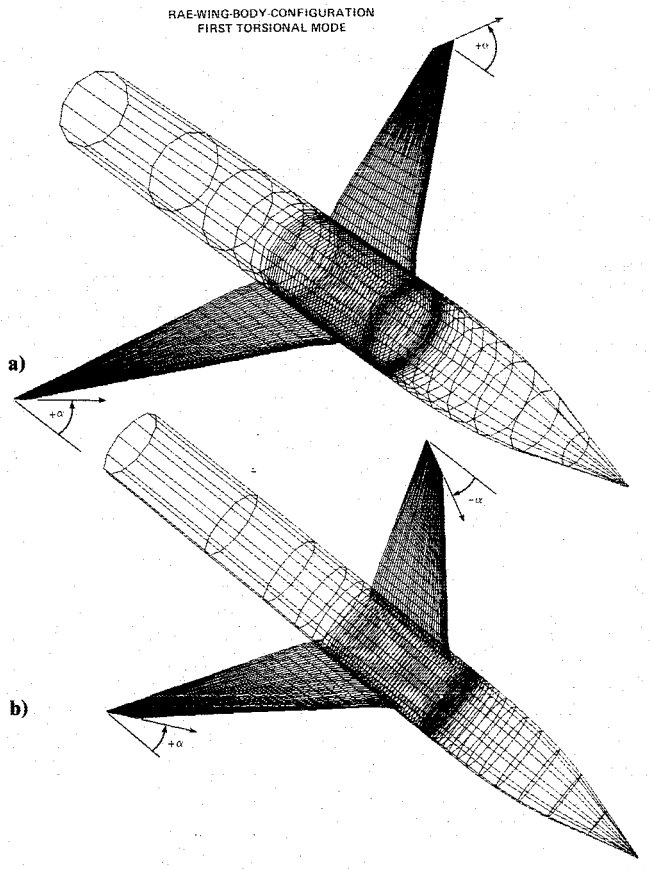

Fig. 15 Twisting modes of the RAE wing-body configuration: a) symmetric; and b) antisymmetric.

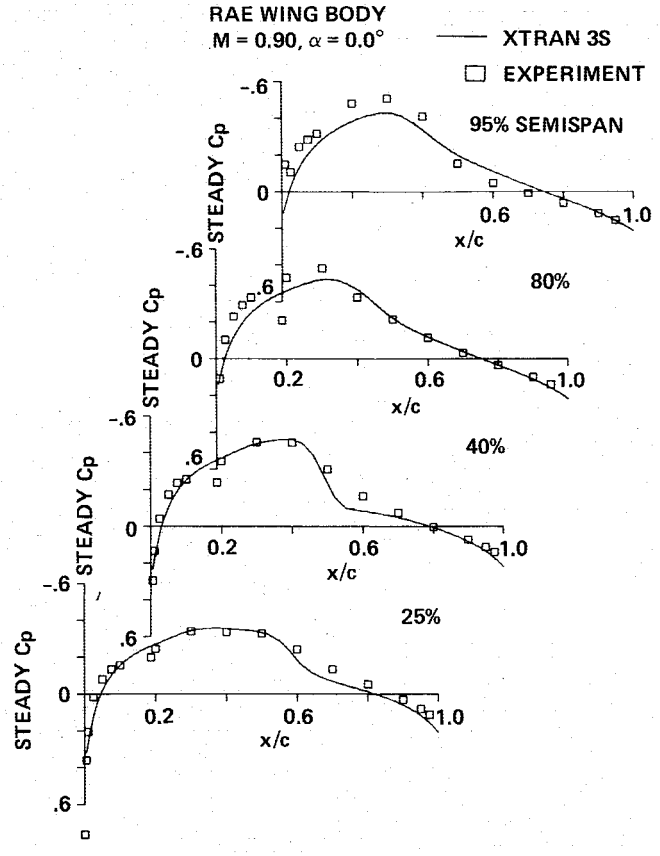

Fig. 14 Steady pressure distributions on the wing of the RAE wing-body configuration.

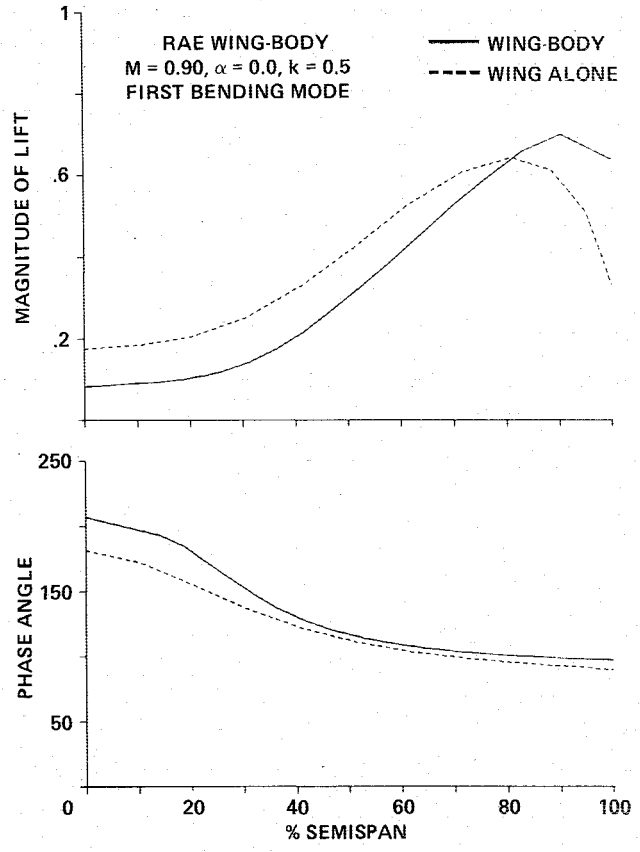

Fig. 16 Comparison of unsteady lift coefficients between wing-body and wing-alone configurations.

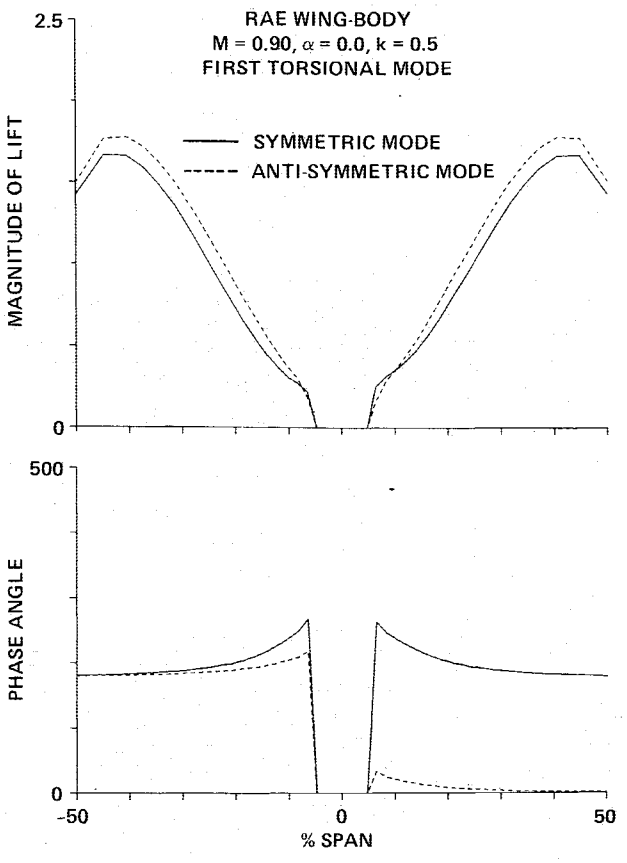

Fig. 17 Comparison of unsteady lift coefficients between symmetric and antisymmetric twisting modes for the RAE wing-body configuration.

bending and first-torsional modes were considered. Figure 15 shows first-torsional symmetric and antisymmetric modes of the RAE wing-body configuration. Figure 16 shows the symmetric and antisymmetric first-torsional modes. All computations were made at a Mach number of 0.90 for wings oscillating at a reduced frequency of 0.5. Figure 16 shows the unsteady lift coefficients for the RAE wing-body configuration and an equivalent RAE wing mounted on a wall. The presence of the body shifts both the lift magnitude and the phase-angle curve significantly enough to affect the aeroelastic computations.

Figure 17 shows unsteady lift coefficients for symmetric and antisymmetric twisting modes. The antisymmetric mode increases the magnitude and decreases the phase angle of the lift coefficient. The influence of the antisymmetric twisting mode on the unsteady lift coefficient is present throughout the wing span, particularly in magnitudes. When compared to the bending mode (results not shown here), the twisting mode has more influence on the unsteady pressures, a result of the antisymmetry. Such differences owing to antisymmetry can significantly influence the aeroelastic characteristics of an aircraft.

Conclusions

A procedure has been developed for computing unsteady, transonic aerodynamic loads on full-span-wing-body configurations. Keeping practical aeroelastic applications in view, which require computational times that are about two orders of magnitude greater than those required for unsteady computations for the same configuration, the transonic small-disturbance equations are used to model the flow. Steady computations on a wing-cylinder configuration compare well with other computations. Steady computations for a wing-finite-body configuration compare well with experimental results. Unsteady computations for symmetric modes compare favorably in trend with the available experimental data on the same wing without the body. Significant differences that can affect aeroelastic computations were found in the unsteady pressures between symmetric and antisymmetric modes. Although for the purposes of validation antisymmetric modes were used, the present development is valid for arbitrary asymmetric modes. Since the present study models the full span of the wing, unsteady transonic flows associated with asymmetric modes of aircraft carrying stores and asymmetric configurations such as the oblique wing can be simulated successfully.

Acknowledgments

This work was supported through fundings from the Air Force Wright Aeronautical Laboratories of Wright Patterson Air Force Base, and it was monitored by Mr. Larry Huttsell and Mr. Dale Cooley of the Aeroelastic Branch in the Structure and Dynamics Division of the Flight Dynamic Laboratory. The authors appreciate many helpful suggestions made by Mr. Larry Huttsell during the course of this work.

References

[1]Magnus, A. E. and Epton, M. E., "PANAIR—A Computer Program for Predicting Subsonic or Supersonic Linear Potential Flows About Arbitrary Configurations Using a Higher Order Panel Method," Vol. I. Theory Document (Version-1), NASA CR-3251, 1980.

[2]Boppe, C. W., "Computational Transonic Flow About Realistic Aircraft Configurations," AIAA Paper 78-104, Jan. 1978.

[3]Flores, J., Holst, T. L., Gundy, K. L., and Reznick, S. G., "Transonic Navier-Stokes Solutions for a Fighter-Like Configuration," AIAA Paper 87-0032, Jan. 1987.

[4]Ashley, H., "Role of Shocks in the 'Sub-Transonic' Flutter Phenomenon," *Journal of Aircraft*, Vol. 17, March 1980, pp. 187–197.

[5]Guruswamy, G. P., Goorjian, P. M., and Tu, E. L., "Unsteady Transonics of a Wing with Tip Store," *Journal of Aircraft*, Vol. 23, Aug. 1986, pp. 662–668.

[6]Huttsell, L. J. and Cooley, D. E., "The Background and Status of the Joint Air Force/NASA Transonic Unsteady Aerodynamic Program (XTRAN3S)," Air Force Wright Aeronautical Labs., Wright Patterson Air Force Base, OH, AFWAL-TM-86-154-FIBRC, Jan. 1986.

[7]Guruswamy, G. P. and Goorjian, P. M., "An Efficient Coordinate Transformation Technique for Unsteady Transonic Aerodynamic Analysis of Low Aspect Ratio Wings," AIAA Paper 84-0872-CP, May 1984.

[8]Rizzetta, D. P. and Borland, C. J., "Numerical Solution of Three-Dimensional Unsteady Transonic Flow Over Wings Including Inviscid/Viscous Interaction," AIAA Paper 82-0352, Jan. 1982.

[9]Guruswamy, G. P. and Goorjian, P. M., "Transonic Aeroelastic Analysis of the B-1 Wing," *Journal of Aircraft*, Vol. 23, July 1986, pp. 547–553.

[10]Bailey, R. F. and Ballhaus, W. F. "Comparisons of Computed and Experimental Pressures for Transonic Flows About Isolated Wings and Wing-Fuselage Configurations," NASA-SP-347, 1975.

[11]Mason, W. H., Mackenzie, C., Stern, M., Ballhaus, W. F., and Frick, J., "An Automated Procedure for Computing the Three-Dimensional Transonic Flow Over Wing-Body Combinations, Including Viscous Effects," Air Force Flight Dynamic Lab., Wright Patterson Air Force Base, OH, Rept. AFFDL-TR-77-122, Vol. I, Feb. 1978.

[12]Batina, J. T., "Unsteady Transonic Flow Calculations for Wing-Fuselage Configurations," AIAA Paper 86-0862-CP, May 1986.

[13]Treadgold, D. A., Jones, A. F., and Wilson, K. H., "Pressure Distribution Measured in the RAE 8 ft × 6 ft Transonic Wind Tunnel on RAE Wing 'A' in Combination with an Axi-Symmetric Body at Mach Numbers of 0.4, 0.8, and 0.9," *Experimental Data Base for Computer Program Assessment*, AGARD-AR-138, May 1979.

[14]Yoshihara, H., "Formulation of the Three-Dimensional Transonic Unsteady Aerodynamic Problem," Wright Patterson Air Force Base, OH, Rept. AFFDL-TR-79-3030, Feb. 1979.

[15]Klunker, E. B. and Newman, P. A., "Computation of Transonic Flow About Lifting Wing-Cylinder Combinations," *Journal of Aircraft*, Vol. 11, April 1974, pp. 254–256.

[16]Lessing, H. C., Troutman, J. L., and Menees, G. P., "Experimental Determination of the Pressure Distribution on a Rectangular Wing Oscillating in First-Bending Mode for Mach Numbers from 0.24 to 1.30," NASA TN D-344, 1960.